

# Spontaneous emission in the near-field of 2D photonic crystals

**A. Femius Koenderink**

*Laboratory of Physical Chemistry, Swiss Federal Institute of Technology (ETH), 8093 Zurich, Switzerland*

**Maria Kafesaki**

*IESL, Foundation for Research and Technology Hellas (FORTH), P.O. Box 1527, 71110 Heraklion, Crete, Greece*

**Costas M. Soukoulis**

*Ames Laboratory, Iowa State University, Ames, Iowa 50011, and IESL, FORTH, P.O. Box 1527, 71110 Heraklion, Greece, and Dept. of Materials Science and Technology, University of Crete, Greece*

**Vahid Sandoghdar**

*Laboratory of Physical Chemistry, Swiss Federal Institute of Technology (ETH), 8093 Zurich, Switzerland*

Compiled November 8, 2018

We show theoretically that photonic crystal membranes cause large variations in the spontaneous emission rate of dipole emitters, not only inside but also in the near-field above the membranes. Our three-dimensional finite difference time-domain calculations reveal an inhibition of more than five times and an enhancement of more than ten times for the spontaneous emission rate of emitters with select dipole orientations and frequencies. Furthermore we demonstrate theoretically, the potential of a nanoscopic emitter attached to the end of a glass fiber tip as a local probe for mapping the large spatial variations of the photonic crystal local radiative density of states. This arrangement is promising for on-command modification of the coupling between an emitter and the photonic crystal in quantum optical experiments. © 2018 Optical Society of America

*OCIS codes:* 130.130, 160.0160, 180.5810, 270.5580

It is well known that the rate of spontaneous emission can be controlled by the geometry of the medium surrounding the fluorescent species. In particular, many recent research efforts have been devoted to studying spontaneous emission in photonic crystals.<sup>1–3</sup> The quantitative interpretation of these experiments, however, remains frustrated by lack of detailed information about many parameters that strongly affect the emission dynamics. These include the exact position of the emitters on the subwavelength scale and the orientation of the emission dipole moments, as well as systematic effects such as surface-induced quenching<sup>4</sup> or other chemical or electronic surface phenomena. An ideal arrangement would require accurate placement of a single emitter at an arbitrary location in a photonic crystal (PC). Very recently Badolato *et al.* have achieved this by precise fabrication of a PC structure around a given semiconductor emitter.<sup>5</sup> In this Letter we discuss the *in-situ* control of the position and thereby modification of the spontaneous emission rate of a single emitter close to or in a two-dimensional PC slab.

Two-dimensional (2D) photonic crystals fabricated in thin semiconductor membranes promise to achieve many of the long-standing goals of photonic band gap materials. Indeed, recently it has been demonstrated that it is possible to achieve very high-Q and low mode volume cavities in these structures.<sup>6,7</sup> Due to their planar nature, PC membranes can be easily accessed by sub-wavelength probes such as optical fiber<sup>9</sup> or atomic force microscope tips.<sup>16</sup> Motivated by this opportunity, we in-

vestigate the prospects of coupling between a PC and nanoscopic optical emitters located at the end of sharp probes.<sup>10–12</sup> Although 2D crystals do not yield a zero density of states, we show that both inside and in the near-field above a PC membrane the emission rate of properly oriented dipoles can be strongly modified. We show that the nanometer accuracy in scanning probe positioning allows direct mapping of the dependence of the emission rate on the spatial coordinates of the subwavelength emitter.

We have used the three-dimensional Finite-Difference Time-Domain (FDTD) method<sup>8,13,14</sup> to calculate the local radiative density of states (LRDOS), accounting for the position dependence of the photon states available for fluorescent decay of a quantum emitter.<sup>15</sup> This calculation relies on the fact that the LRDOS appearing in the formulation of Fermi's Golden Rule for the spontaneous emission rate, also describes the total emitted power of a classical point-dipole antenna run at a fixed current.<sup>8</sup> We consider semiconductor membranes with dielectric constant  $\epsilon = 11.76$  and thickness  $d = 250$  nm, surrounded by up to  $1 \mu\text{m}$  of air above and below. We take the membrane to contain a hexagonal array of holes with radius  $r = 0.3a$  at a lattice spacing of  $a = 420$  nm. Such a structure possesses a band gap in the range  $a/\lambda = 0.25$  to  $0.33$  for the transverse electric (TE) mode where the electric field is parallel to the plane of the membrane. The ratio  $a/\lambda$  is used as normalized frequency units throughout our work. We used discretization with 14 or 20 points per lattice constant and employed volume-averaging of

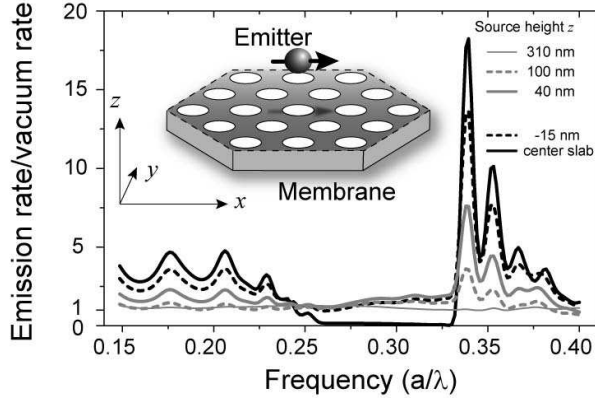


Fig. 1. Emission rate normalized to the vacuum rate versus frequency for an  $x$ -oriented dipole in the central hole of a PC membrane (details in text). Black lines correspond to dipoles in the slab ( $z < 0$ ) and gray lines to dipoles above the slab ( $z > 0$ ), as listed in the legend.

the dielectric constant to reduce staircasing errors.<sup>16</sup> We considered finite hexagonally shaped PC structures up to 25 holes across, terminated by the unperforated slab extending into Liao's absorbing boundary conditions. By broadband temporal excitation of the dipole, we simulated the emission power spectrum over a wide frequency range. After dividing the resulting spectrum by that of an identically excited dipole in vacuum, we obtained the LRDOS normalized to the vacuum LRDOS.<sup>14</sup>

For an emitter half way deep in a PC membrane, the solid black spectrum in Fig. 1 shows a strong inhibition of fluorescence by over a factor of 7 in the band gap as compared to its vacuum rate. In this case the dipole was laterally centered in the structure, and its orientation was chosen in the  $x$ -direction (cf. Fig. 1). The slab was taken to be  $13a$  across, and we verified that no significant further reduction of the emission rate was obtained if we increased the size of the structure. However, the magnitude of the enhancement at the blue edge of the gap, as well as the Fabry-Pérot oscillations at frequencies below the gap depend on the finite size of the PC structure. For all tested structures wider than 7 holes across, we find emission enhancements larger than a factor of 15, representing a jump of two orders of magnitude as compared to the LRDOS for frequencies in the gap.

Given the inherent strong modulation of the dielectric constant in a PC structure, it is particularly interesting to examine the lateral dependence of the spontaneous emission rate. Figure 2(a) shows a contour plot of the LRDOS modification for an  $x$ -oriented dipole midway in the slab depth versus emission frequency and for lateral locations along a trajectory that traces the irreducible part of the unit cell (Fig. 2(d)). The emission is inhibited in the band gap at all positions whereas outside the gap we observe Fabry-Pérot modulations together with enhancement at the low and high frequency edges. The enhancement of the emission occurs especially on the high

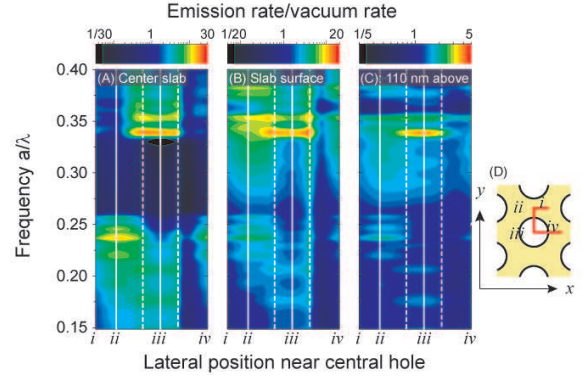


Fig. 2. (color) Emission rate normalized to the vacuum rate for an  $x$ -oriented dipole (a) in the mid-depth, (b) on the surface and (c) 110 nm above the PC membrane as a function of frequency and position along the trajectory indicated by the red line in (d). The trajectory traces the edges of the irreducible part of the unit cell. The dashed lines mark the borders between air hole and dielectric. The logarithmic color scales are shown on top.

frequency edge of the gap (the ‘air band’) for dipoles in air holes, and predominantly at the low frequency edge (the ‘dielectric band’) for dipoles in the dielectric.

Next, we ask whether it is possible to capture these effects by scanning an emitter just above the PC slab. Different spectra in Fig. 1 show the LRDOS modification of a dipole laterally centered in the structure but at various heights  $z$  above the membrane. In addition Fig. 2(b) and (c) display the modification of the LRDOS for the dipole right at the crystal-air interface and at 110 nm above this plane. These data reveal that as  $z$  increases, the inhibition and enhancement reduce in size. To examine this distance dependence more closely, in Fig. 2 we plot the normalized emission rate as a function of the distance between the dipole and the membrane surface for three key frequencies  $a/\lambda = 0.23, 0.28$  and  $0.34$  just below, in, and just above the band gap, respectively. Evidently, the inhibition diminishes for emitters located above the slab. In contrast, enhancements persist at the blue edge of the gap even if the dipole is lifted into air above the membrane. Figures 2 and 3 let us conclude that it is possible to enhance the spontaneous emission rate by a factor of 5 to 10 if the emitter position is controlled to within 50 nm above the PC membrane. Note that the emission of a dipole near a simple homogeneous dielectric slab is also enhanced, due to coupling to the guided modes. However, at the gap edges the PC causes a further strong enhancement of the LRDOS.<sup>17</sup>

The required resolution and control for mapping the modification of the emission rate can be achieved by scanning a subwavelength emitter attached to the end of a sharp tip.<sup>10–12</sup> A crucial question arises as to the effect of the tip on the LRDOS. To estimate this effect, we have calculated the LRDOS for sources embedded inside cylindrical tips of diameter 125 nm pushed 130 nm

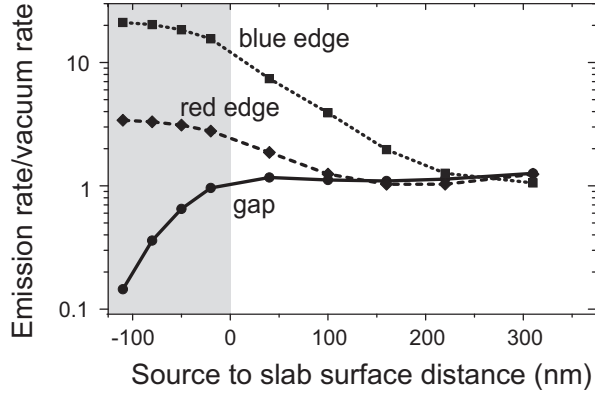


Fig. 3. Emission rate modification as a function of the height of a dipole above the PC membrane. Circles, diamonds and squares show data for  $a/\lambda = 0.23, 0.28, 0.34$ , corresponding to frequencies below, in and above the gap, respectively. The shaded region shows the range of positions  $-125 < z < 0$  nm in the membrane.

into the central hole of the PC structure. We find that the influence of the PC structure on the spectrum of LRDOS enhancement and inhibition is unchanged for the system of emitters embedded in glass ( $\epsilon \lesssim 2.25$ ). In contrast, tips of very high-index material such as silicon fundamentally change the LRDOS spectrum, leading to the creation of a low-Q localized defect mode from the band edge due to the addition of dielectric material.<sup>16</sup> The presence of a silicon tip causes an overall reduction of the gap depth and an increase and red-shift of the rate enhancement at the blue edge of the gap. Suitable probes of the LRDOS in photonic crystal membranes are therefore emitters inside low index tips.

Although optical detection of single emitters has become possible for some systems, many applications such as the realization of a nanolaser would benefit from coupling an ensemble of emitters to a PC. Furthermore, nanoscopic ensembles are more readily available than single emitter systems. Thus, we have also considered the modification of the spontaneous emission rate for a subwavelength ensemble of randomly oriented dipoles. Note that because the LRDOS is essentially unchanged for the TM polarization, dipolar components normal to the slab reduce the visibility of lifetime effects. We have considered over 25 in-equivalent dipole orientations (corresponding to over 300 orientations in  $2\pi$  solid angle) in the central air hole and have calculated the corresponding LRDOS and luminescence extraction efficiency.<sup>8,17,18</sup> We find that in general, the time-resolved flux of fluorescence photons extracted from the slab follows a significantly non-single exponential decay behavior. Nonetheless, the mean decay constant reveals inhibition by a factor three, and enhancement by a factor five compared to vacuum. The observation of inhibition is facilitated by the increase of the emission extraction efficiency for in-plane dipoles from  $\sim 20\%$  for frequencies below the gap to  $> 80\%$  in the gap.<sup>8,18</sup>

In conclusion, we have shown that strong inhibition and enhancement of emission can be achieved for emitters well inside photonic crystal membranes while a significant level of enhancement persists even in the near field above the structures. Since these results also hold for emitters embedded in nanoscopic dielectric probes, scanning probe technologies can be promising for on-command spontaneous emission control. An important advantage of emitters inside such probes is that they are shielded from unwanted interactions, and can be calibrated by simply retracting the probe from the structure.

This work was funded by the Deutsche Forschungsgemeinschaft (DFG) through focus program SP1113 and by ETH Zürich. Vahid Sandoghdar can be reached by e-mail at vahid.sandoghdar@ethz.ch.

## References

1. C. M. Soukoulis, ed., *Photonic crystals and light localization in the 21<sup>st</sup> century* (Kluwer Academic Publishers, Dordrecht, 2001).
2. P. Lodahl, A. F. van Driel, I. S. Nikolaev, A. Irman, K. Overgaag, D. Vanmaekelbergh, and W. L. Vos, *Nature* **430**, 654–657 (2004).
3. S. P. Ogawa, M. Imada, S. Yoshimoto, M. Okano, and S. Noda, *Science* **305**, 227–229 (2004).
4. P. V. Kamat, *Chem. Rev.* **93**, 267–300 (1993).
5. A. Badolato, K. Hennessy, M. Atatüre, J. Dreiser, E. Hu, P. M. Petroff, and A. Imamoglu, *Science* **308**, 1158–1161 (2005).
6. T. Yoshie, A. Scherer, J. Hendrickson, G. Khitrova, H.M. Gibbs, G. Rupper, C. Ell, O.B. Shchekin, and D.G. Deppe, *Nature* **432**, 200–203 (2004).
7. Y. Akahane, T. Asano, B. S. Song, and S. Noda, *Nature* **425**, 944–947 (2003).
8. R. K. Lee, Y. Xu, A. Yariv, *J. Opt. Soc. Am. B* **17**, 1438–1442 (2000).
9. P. Kramper, M. Kafesaki, C. M. Soukoulis, A. Birner, F. Müller, U. Gösele, R. B. Wehrspohn, J. Mlynek and V. Sandoghdar, *Opt. Lett.* **29**, 174–176 (2004).
10. J. Michaelis, C. Hettich, J. Mlynek, and V. Sandoghdar, *Nature* **405**, 325–328 (2000).
11. S. Kühn, C. Hettich, C. Schmitt, J. P. H. Poizat, and V. Sandoghdar, *J. Microsc.* **202**, 2 (2001).
12. V. Zwiller, T. Aichele, F. Hatami, W. T. Masselink, and O. Benson, *Appl. Phys. Lett.* **86**, 091911 (2005).
13. A. Taflov and S.C. Hagness, *Computational Electrodynamics: The Finite-Difference Time-Domain Method* (2nd ed., Artech House, Boston, MA, 2000).
14. C. Hermann and O. Hess, *J. Opt. Soc. Am. B* **19**, 3013–3018 (2002).
15. R. Sprik, B. A. van Tiggelen, and A. Lagendijk, *Europhys. Lett.* **35**, 265–270 (1996).
16. A. F. Koenderink, M. Kafesaki, B. C. Buchler, and V. Sandoghdar, submitted (2004). e-print <http://arxiv.org/abs/cond-mat/0412394>.
17. A. F. Koenderink, M. Kafesaki, C. M. Soukoulis, and V. Sandoghdar, in preparation (2005).
18. S. Fan, P. R. Vileneuve, J. D. Joannopoulos and E. F. Schubert, *Phys. Rev. Lett.* **78**, 3294–3297 (1997).